Small-Signal Modeling and Analysis of Current-Mode Control for Multiple-Output Forward Converters

Qing Chen and Fred C. Lee
Virginia Power Electronics Center
The Bradley Department of Electrical Engineering
Virginia Polytechnic Institute and State University
Blacksburg, VA 24061, U.S.A.

Milan M. Jovanovic
Delta Research Lab., Inc.
1861 Pratt Drive
Blacksburg, VA 24060, U.S.A.

Abstract *-- A small-signal model for multiple-output forward converter with current model control is derived. The model can accurately predict the small-signal characteristics for current mode control. Both theoretical and experimental results show that the power stage pole-zero relative positions, which are critical to the compensator design, are not affected by introducing current mode control.*

I. Introduction

Current-mode control is often used in conjunction with weighted voltage control and coupled inductors in a multiple-output converter (MOC). In spite of wide application of current-mode control in MOCs, the small-signal characteristics of current-mode control for the MOCs are not well understood. The published work on current-mode control for MOCs is limited to dc regulation analysis [1]. There is no small-signal model available for analysis and design when current-mode control is applied. The purpose of this paper is to present a small-signal analysis and provide design insight for the application of current-mode control to MOCs.

First, a small-signal model for MOCs with current-mode control is established. The model includes the effects of weighted control and coupled inductors, which distinguish MOCs from their single-output counterparts. The model is able to predict some unique characteristics of current-mode control, such as subharmonic oscillation and removal of power stage pole to high frequency. The design considerations are discussed. The derived small-signal model is experimentally verified on a dual-output forward converter.

II. Small-Signal Model for Current-Mode Control

Figure 1 shows a multiple-output forward converter with current-mode control. According to its function, the circuit can be decomposed into three parts: (1) the power stage, which is the same as the voltage-mode control, and its small-signal model was presented in [2]; (2) the current-mode control stage, which includes the information of the sensed currents, the feedforward and feedback gains; and (3) the compensator stage, which is required for both voltage- and current-mode control but is different for voltage- and current-mode control. This section is focused on part (2) - derivation of the current-mode control. The small-signal characteristics and design issues are discussed in next two sections.

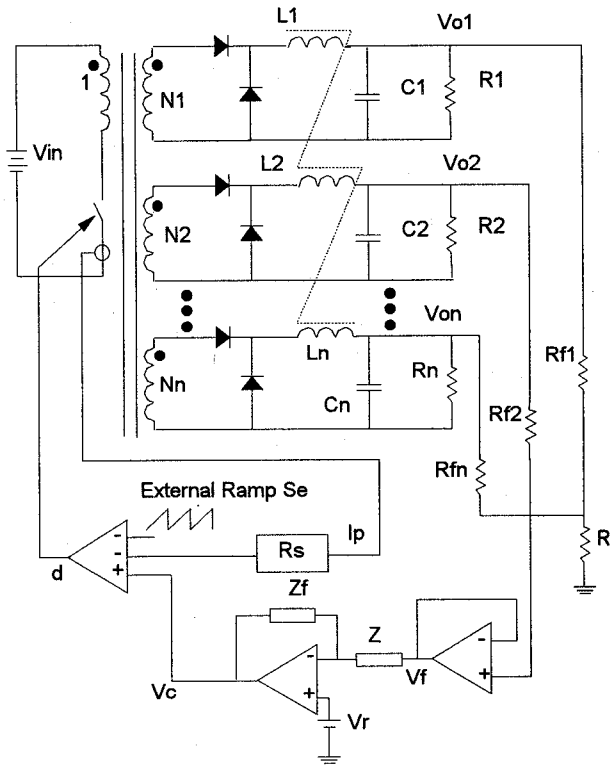

Fig. 1. A multiple-output forward converter with current-mode control with WVC. *Usually, the primary current, which contains the information of all the load currents, is sensed to implement the current mode control.*

To provide design insight, the analysis is performed for a dual-output forward converter. The basic concept can be easily extended to other topologies with an arbitrary number of outputs.

This work was supported in part by Delta Electronic Ind. Co., Ltd., Taiwan, and the Virginia Center fro Innovative Technology.

0-7803-1859-5/94/$4.00 © 1994 IEEE

A. Modulation and Sampling Gains

The duty cycle, d, for control of the converter is typically generated with a control voltage and a reference ramp clocked at the desired switching frequency. For single output converter, the current waveform, in conjunction with an external ramp, provides the ramp of the modulator. The modulator gain of the circuit, F_m, is [3]

$$F_m = \frac{1}{(S_n + S_e)T_s}, \tag{1}$$

where T_s is the switching period, S_n is the on-time slope of the sensed-current waveform, and S_e is the external ramp which provides design flexibility and stabilizes the current feedback loop [4-6]. For a MOC, since the feedback signal is derived from the primary side, it contains the information about both inductor currents. The on- and off-time slopes of the primary current can be derived from the generic current-mode cell for MOC, as shown in Fig. 2. For a multiple-output forward converter, the on-time slope, S_{np}, and off-time slope, S_{fp}, of the sensed current are

$$S_{np} = R_s(N_1 S_{n1} + N_2 S_{n2}), \text{ and} \tag{2}$$

$$S_{fp} = R_s(N_1 S_{f1} + N_2 S_{f2}), \tag{3}$$

where S_{ni} and S_{fi} are the on- and off-time slopes of the currents through the output filter inductors, and L_1 and L_2, respectively, and are given by:

$$S_{ni} = \frac{(N_i L_j - N_j M)V_{oni}}{L_1 L_2 - M^2}, \quad i,j=1,2, \quad i \neq j, \text{ and} \tag{4}$$

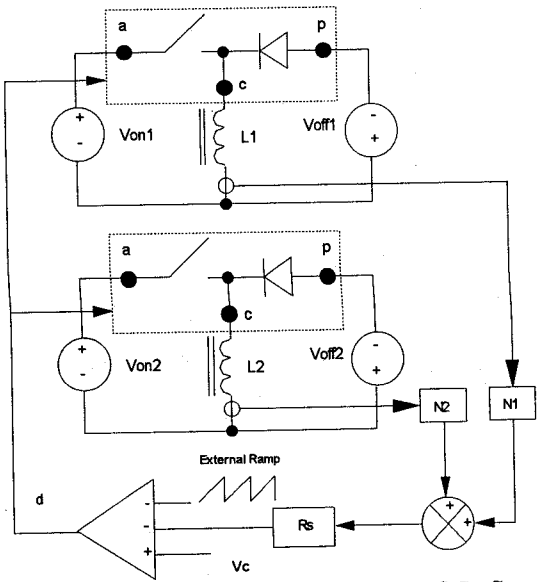

Fig. 2. Generic current-mode cell for MOC. *Since the generic current-mode cell is invariant for different topologies, it can also be used for other converters with current-mode control. Notice that the inductors are coupled on the same core.*

$$S_{fi} = \frac{(N_i L_j - N_j M)V_{offi}}{L_1 L_2 - M^2}, \quad i,j=1,2, \quad i \neq j. \tag{5}$$

where V_{oni} and V_{offi} are the on- and off-time voltages across the output filter inductors.

Equations (2) and (3) include the effects of the coupled inductors which are unique to MOCs. Substituting Eq. (2) into Eq. (1) gives the expression of the modulator gain.

Since current-mode control exhibits characteristics which can only be explained with discrete model [3], the constant frequency current-mode control converter can be considered a sample-and-hold system with the sampling instant occurring at the intersection of the current signal and the reference voltage. The transfer function of the sampling-and-hold can be approximated by a 2nd-order system [6]:

$$H_e(s) \approx 1 + \frac{s}{\omega_n Q_z} + \frac{s^2}{\omega_n^2} \tag{6}$$

where: $Q_z = -\frac{2}{\pi}$ and $\omega_n = \frac{\pi}{T_s}$.

B. Feedback and Feedforward Gains

The average inductor currents of the circuit are related to the instantaneous current through the current slopes which are affected by input and output voltages. The feedforward gains from the input voltage and the feedback gains from the output voltages are used to model this dependence. Though the feedforward and feedback gains can be derived from Fig. 1, their expressions depend on the specific topology. Therefore, they have to be derived for each circuit. The generic current-mode cell for MOCs shown in Fig. 2 is invariant for different topologies, since the dependence of the inductor current is not directly associated with the input and output voltages, but rather with the on- and off-time voltages across the inductor. The on- and off-time voltages across the inductor are merely the linear combinations of the input and output voltages. The small-signal model of the current cell for the MOC is shown in Fig. 3.

Referring to the generic current-mode cell in Fig. 2, the relations between the duty cycle, d, and the on- and off-time voltages across the inductors can be derived as:

$$d = \frac{v_{off1}}{v_{on1} + v_{off1}} = \frac{v_{off2}}{v_{on2} + v_{off2}}, \text{ and} \tag{7}$$

$$d' = \frac{v_{on1}}{v_{on1} + v_{off1}} = \frac{v_{on2}}{v_{on2} + v_{off2}}. \tag{8}$$

The steady-state waveforms pertinent to the derivation are given in Fig. 4, from which the average value of the sum of inductor currents referred to the primary is derived as:

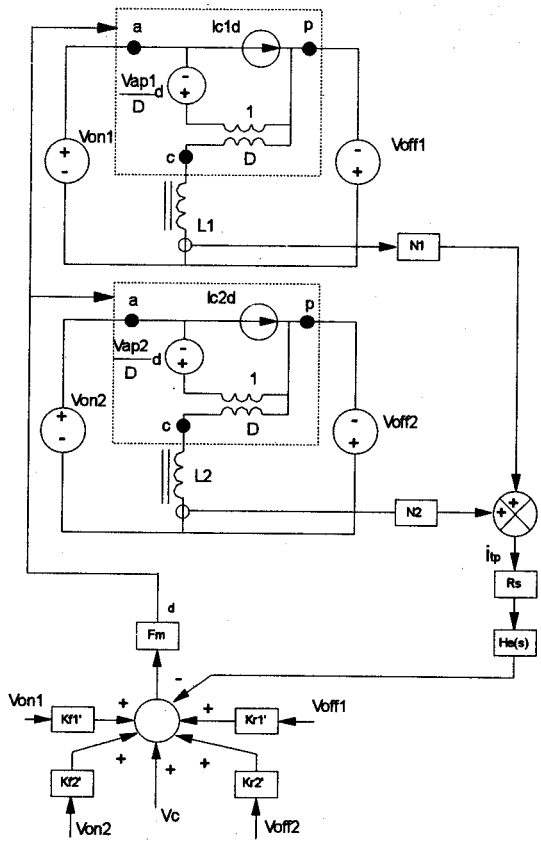

Fig. 3. Small-signal model for the generic current cell. *For a forward converter, each on-time voltage is the difference between the secondary voltage and the corresponding output voltage, whereas each off-time voltage is the corresponding output voltage.*

$$R_s <i_{tp}> = v_c - dT_s S_e - \frac{S_{fp} d' T_s}{2}. \tag{9}$$

Substitution of Eqs. (7) and (8) into Eq. (9) yields

$$R_s <i_{tp}> = v_c \frac{S_e T_s v_{off1}}{v_{on1} + v_{off1}} - \frac{S_{fp} T_s}{2} \frac{v_{on1}}{(v_{on1} + v_{off1})}. \tag{10}$$

Perturbing the average current with respect to the on-time voltage v_{on1} gives:

$$\frac{R_s <i_{tp}>}{v_{on1}} = \frac{DT_s S_e}{V_{ap1}} - \frac{D^2 T_s S_{fp}}{2V_{off1}}. \tag{11}$$

The same quantity can be obtained from Fig. 3 by perturbing v_{on1} and assuming v_{on2}, v_{off1}, and v_{off2} to be zero. It is noticed that the inductors are shorted under dc condition. Then the following two equations are obtained:

$$d = F_m (K'_{f1} v_{on1} - <i_{tp}> R_s), \tag{12}$$

$$v_{on1} + \frac{V_{ap1}}{D} d = 0. \tag{13}$$

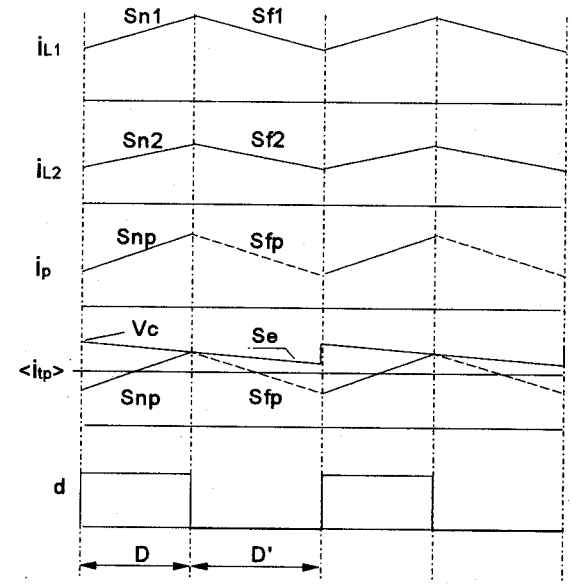

Fig. 4. Steady-state waveforms for current-mode control. *The variables are defined as: i_{Li} - inductor current; i_p - primary current; i_{tp} - sum of the inductor currents referred to the primary; S_{ni} (S_{fi}) - on-time (off-time) inductor current slope; S_{np} (S_{fp}) - on-time (off-time) slope of the sum of the inductor currents referred to the primary; S_e - external ramp slope; v_c - control voltage.*

Solving these two equations for the ratio of the sensed current and the on-time voltage v_{on1} yields:

$$\frac{R_s <i_{tp}>}{v_{on1}} = \frac{D}{V_{ap1} F_m} + K'_{f1}, \tag{14}$$

Let Eq. (11) be equal to Eq. (14):

$$\frac{DT_s S_e}{V_{ap1}} - \frac{D^2 T_s S_{fp}}{2V_{off1}} = \frac{D}{V_{ap1} F_m} + K'_{f1}. \tag{15}$$

The feedforward gain K'_{f1} is solved as:

$$K'_{f1} = -\frac{D^2 T_s}{V_{off1}} (S_{np} + \frac{S_{fp}}{2}). \tag{16}$$

The feedback gain from the off-time voltage, v_{off1}, to the control can be derived in the similar manner, and is given as follows:

$$K'_{r1} = \frac{D'^2 T_s S_{np}}{2V_{on1}}. \tag{17}$$

Swapping the subscript from 1 to 2, the feedforward and feedback gains K'_{f2} and K'_{r2} are obtained.

For a forward converter, the on- and off-time voltages are

$$V_{oni} = V_{in} N_i - V_{Di} - V_{oi}, \qquad i = 1,2, \tag{18}$$

$$V_{offi} = V_{oi} + V_{Di}, \quad i = 1,2, \tag{19}$$

where V_{Di}'s are the forward voltage drops caused by the rectifier diodes. A feedforward path from the input voltage is provided by the feedforward gain K'_{fi} only. The feedback from the output voltage is provided by both K'_{fi} and K'_{ri}. The feedforward and feedback gains for the forward converter are therefore calculated as:

$$K_{fi} = K'_{fi}, \quad i = 1,2, \tag{20}$$

and the feedback gains are

$$K_{ri} = K'_{ri} - K'_{fi} = \frac{DT_s}{2V_{offi}}[(1+D)S_{np} + DS_{fp}], \quad i = 1,2. \tag{21}$$

Since the inputs for two power channels are derived from the same input voltage, it is more meaningful to express the feedforward gain directly from the input voltage to the duty cycle:

$$K_f = -D^2 T_s (S_{np} + \frac{S_{fp}}{2})(\frac{N_1}{V_{off1}} + \frac{N_2}{V_{off2}}). \tag{22}$$

The derivation of feedforward and feedback gains K_f, K_{r1}, and K_{r2} completes the small-signal model for the MOC with current-mode control, as shown in Fig. 5. A more detailed derivation can be found in [7]

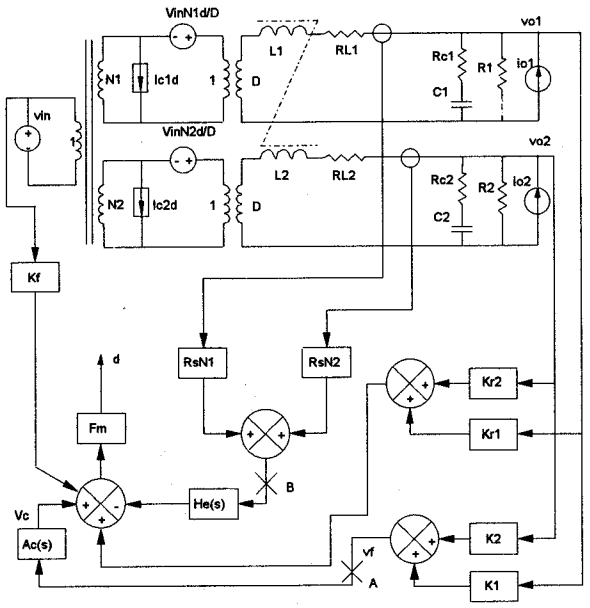

Fig. 5. Complete small-signal model for the MOC with current-mode control. *The feedforward gain represents the effect of the perturbation of the line voltage on the duty cycle. The feedback gains represent the effect of the perturbation of the output voltages on the duty cycle.*

III. Small-Signal Characteristics

The small-signal characteristics of the MOC with current-mode control can be investigated by using the derived model. The small-signal model shown in Fig. 5 was coded into a PSpice program. The parameters of the example circuit are given in Table 1. The operation conditions are V_{in}=150.2 V, V_{o1}=5.1 V, I_{o1}=2.25 A, V_{o2}=11.68 V, I_{o2}=0.73 A, and D=0.34.

Table 1. List of the Circuit Parameters.

N_1	0.107	N_2	0.25
L_1 (μH)	17.8	R_{L1} (Ω)	0.037
L_2 (μH)	96.6	R_{L2} (Ω)	0.12
C_1 (μF)	50	R_{c1}(Ω)	0.0087
C_2 (μF)	24	R_{c2}(Ω)	0.0087
R_{1min} (Ω)	0.333	R_{2min} (Ω)	4
R_{1max} (Ω)	2.5	R_{2max} (Ω)	24
K_1	0.278	K_2	0.093
k	0.89	n_{12}	0.479

A. Current Loop Gain

Current loop gain, defined by breaking the current loop at point B in Fig. 5 with voltage loop open, provides stability information for current-mode control. It is well known that for a single output converter, when the duty cycle of a converter operating under current-mode control exceeds 50%, the inductor current can oscillate until a limit cycle is reached (the phenomenon also referred to as "subharmonic oscillation"). For a MOC, the subharmonic oscillation can also happen once the duty cycle exceeds 50%. The derived small-signal model can accurately predict this phenomenon. Figure 6 shows the current loop gain for the operation with duty cycle, $d=0.5$ without external ramp S_e. The gain of the current loop gain touches *0 dB* at half switching frequency and the corresponding phase is -180°, which means the phase margin is 0°. If the duty cycle is increased further, instability occurs.

B. Control-to-output Transfer Functions

The control-to-output transfer function for each power channel is defined as the ratio of the corresponding output voltage, v_{oi}, and the control voltage, v_c, with current loop closed. Figure 7 shows the measurements and calculations of the control-to-output transfer functions, and they agree well. It can be seen that the nice feature of current-mode control is still preserved for MOCs. By applying current-

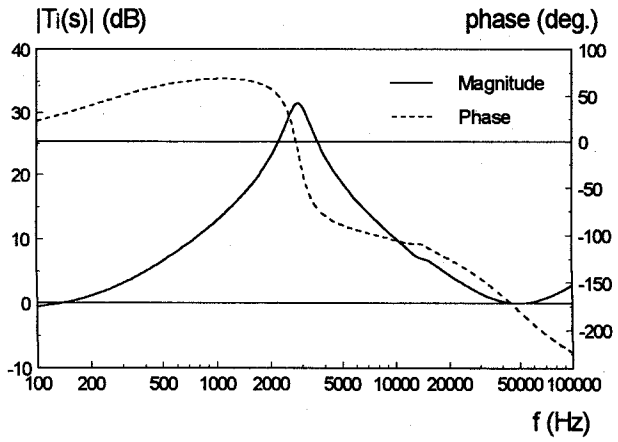

*Fig. 6. **Current-loop gain.** The loop gain clearly shows that when duty cycle is close to 50%, the current loop gain has little phase margin. If duty cycle is increased further, subharmonic oscillation can occur.*

mode control, the low frequency double pole becomes a single pole, which is the same as in the case of single-output converter with current-mode control, followed by a complex zero-pole pair, which is unique to MOCs. At high frequency, the sampling-and-hold effect can be observed. As in the situation when only voltage-mode control is applied, the relative positions of the poles and zeros (here the low frequency single pole and a pair of complex poles and a pair of complex zeros for current-mode control) are crucial for compensator design considerations. For the control-to-output 1 transfer function in Fig. 7 (a), a pair of complex zeros are interlaced with the low frequency single pole and a pair of complex poles. As for the control-to-output 2 transfer function in Fig. 7 (b), however, a pair of complex poles locate between the low frequency single pole and a pair of complex zeros. As a result, the phase drops drastically (almost to -250°) before being brought up by the complex zeros. If the single feedback control scheme is used, it is preferable to feedback the output which has interlaced poles and zeros to realize closed-loop control.

Figure 8 shows the control-to-feedback transfer function, based on which the compensator design is performed. The complex zeros, low frequency single pole, and the high frequency complex poles can be either interlaced or noninterlaced depending upon the values of the weighting factors and coupling coefficient. The pole-zero noninterlaced system has a large phase delay at low frequency; thus it is difficult to achieve high gain and wide bandwidth. To ensure good performance of the converter, it is desirable to have the pole-zero interlaced system.

Compared with the control-to-output and -feedback transfer functions with voltage-mode control only [2], it can be seen that current-mode control does remove one of the low frequency complex double poles to high frequency,

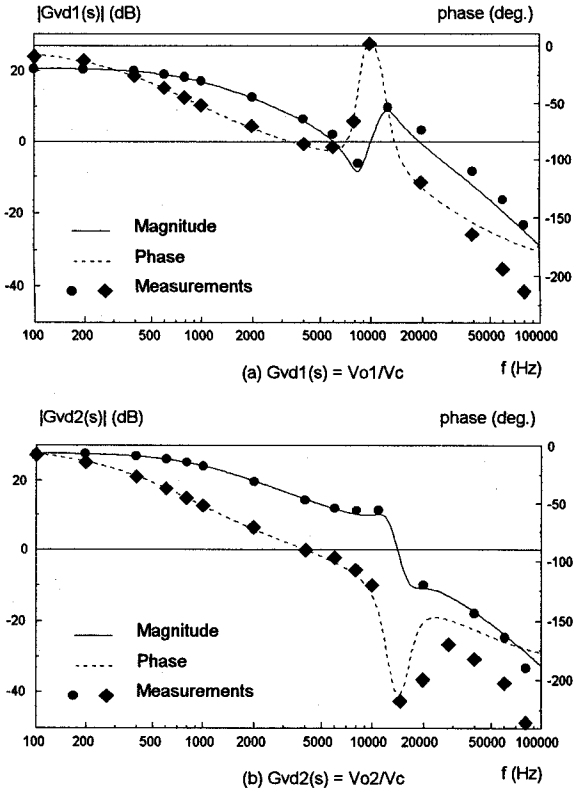

*Fig. 7. **Control-to-output transfer functions with current-loop closed.** At low frequency, the system has one single pole, one pair of complex poles and one pair of complex zeros. Control-to-output 1 transfer function shown in (a) has interlaced poles and zeros, while control-to-output 2 transfer function shown in (b) has non-interlaced poles and zeros.*

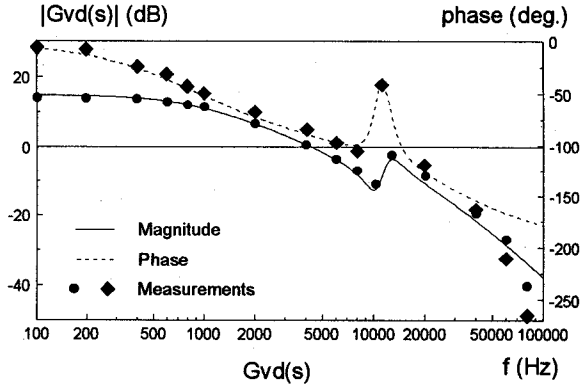

*Fig. 8. **Control-to-feedback transfer function with current-loop closed.** For MOC with weighted-voltage control, the nice feature of current-mode control is still preserved, i.e., the low frequency behaves like a single pole system.*

which results in a single pole at low frequency, but it does not change the relative positions of the poles and zeros. This means that the pole-zero interlacing relation as suggested in

[2] can still be used to design a pole-zero interlaced system even when current-mode control is used.

C. Audio Susceptibilities and Output Impedances

From the derived small-signal model, audio susceptibilities and output impedances (including output transimpedances) can also be calculated.

Figure 9 shows the audio susceptibilities with current loop closed. Comparison with the open-loop audio susceptibilities without current-mode control as given in [7] shows that the audio susceptibilities for both power channels are decreased. From the small-signal model for the MOC with current-mode control in Fig. 5, it can be seen that the perturbation from the line voltage affects the power stage transfer functions in two ways. One is through the power stage small-signal model; the other one is through the feedforward gain, K_f, which is negative. The series connection of the controlled sources with the line voltage makes it possible to eliminate the effects of the line perturbation under certain conditions. Although complete null of audio susceptibilities is not practical due to their sensitivity to the current ramp slops [6], current-mode control can still reduce the effects of the line perturbation on the outputs.

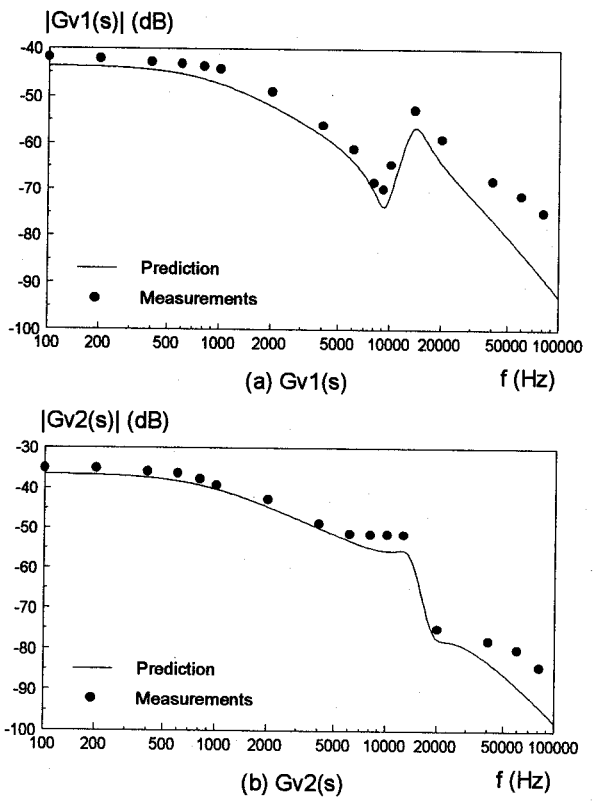

Fig. 9. Open-loop audio susceptibilities with current-loop closed. *The audio susceptibilities are reduced compared with the open-loop audio susceptibilities without current-mode control.*

Figure 10 shows the output impedances with current loop closed. Compared with the output impedances with voltage-mode control only, it can be seen that the output impedances are severely altered, especially at low frequencies. When using voltage-mode control, the open-loop output impedances are basically the resistances of the output filter inductors at the low frequency. Once current-mode control is applied, the low-frequency impedances are increased drastically, because current-mode control makes the output filter inductors behave like current sources. If the compensator for the total feedback voltage, which is the weighted sum of the output voltages, is properly designed, the final output impedances can be attenuated to low values.

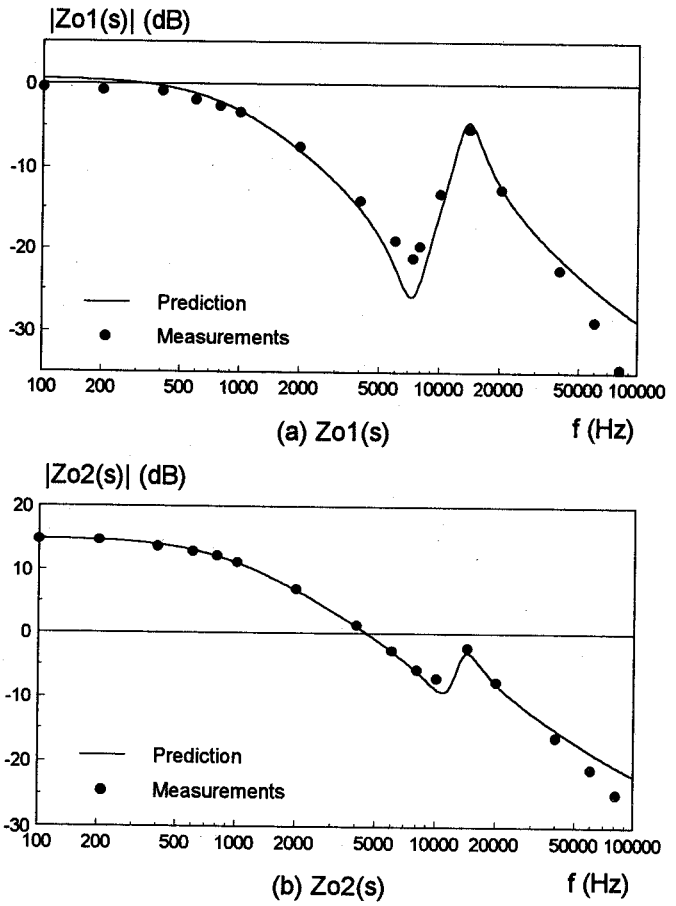

Fig. 10. Open-loop output impedances with current loop closed. *The open-loop output impedances are increased, especially at low frequencies compared with those without current-mode control. Current-mode control makes the output filter inductors behave like current sources.*

If one compares the multiple-output converter with its single-output counterpart, one can find that the small-signal characteristics for both converters are very similar at the low frequencies. The major differences are at the high frequencies. For a single-output converter with current

mode control, the small-signal transfer functions have a low frequency pole plus the double pole at the half switching frequency which is caused by sampling-and-hold. As for the multiple-output converter, the small-signal transfer functions have the same low frequency single pole and the half-switching-frequency double pole. In addition, there is another pair of high-frequency double pole which is caused by the interaction of the coupled inductor and/or weighted voltage control. These effects complicate the small-signal behavior, and therefore the compensator design philosophy is different for the single- and multiple-output converters. The compensator design will be discussed in the next section.

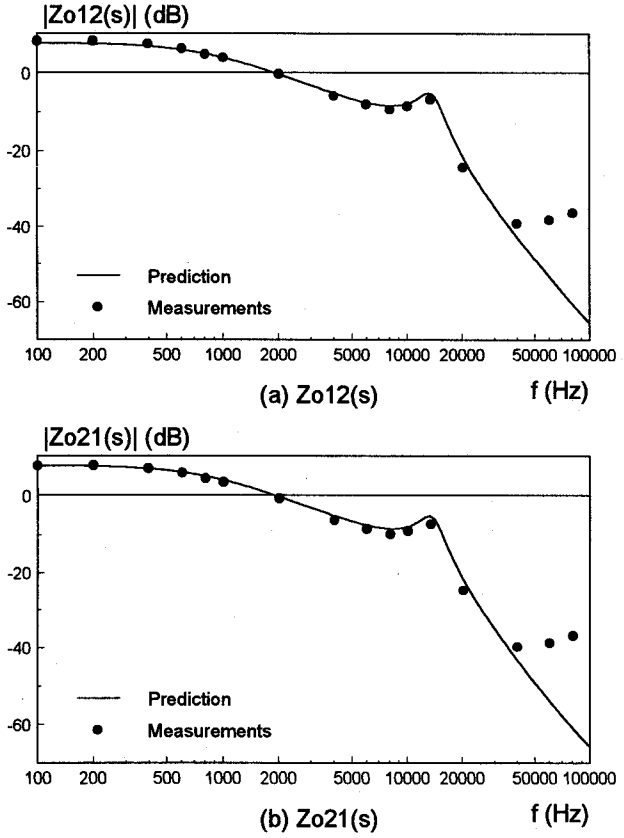

Fig. 11. Open-loop output transimpedances with current loop closed. *The two output transimpedances are exactly the same. Current-mode control does not change the reciprocal nature of the output transimpedances.*

Besides the audio susceptibilities and the output impedances, another important quantity is the output transimpedance, as shown in Fig. 11, which is unique to the multiple-output converter. The output transimpedances characterize the interaction between two power channels. Compared with MOCs with WVC, current-mode control causes the transimpedances to increase drastically at the low frequency. Both predictions and measurements show that the two output transimpedances are exactly the same, which means that current-mode control does not change the reciprocity of the output transimpedances [7].

IV. Design Considerations

For MOCs with current-mode control, the duty cycle-to-output (or feedback) transfer functions at low frequencies are of 3rd order, one single pole plus a pair of complex poles and a pair of complex zeros. The sampling gain is approximated as a second order system with the resonant frequency at half switching frequency. In the compensator design, the distribution of the poles and zeros directly affects the selection of the compensator. For the pole-zero interlaced system, the compensator can assume the form of an integrator plus one pole and one zero. Furthermore, the compensator pole is placed at the ESR zero, and the compensator zero is placed in the vicinity of the first single pole. The compensated system will have a relatively large stability margin and good performance. For pole-zero widely separated and noninterlaced system, the loop must be closed at relatively low frequency to insure enough stability margin; therefore, an integrator has to be used for the compensator. Usually this will yield a poor dynamic response, and therefore it should be avoid by all means. The same pole-zero interlacing relation as given in [2,7] can be used as a design criterion.

Since the small-signal transfer functions of the multiple-output converter exhibit multiple peaks, one should check the small-signal behavior in the vicinities of these peakings. During start-up, the gain characteristics might have multiple crossings over *0-dB* line, which may cause instability.

Figure 12 shows the prediction and measurement of the loop gain with current-mode control. Again, the agreement between the two is good. The primary switch current is sensed with a 1:100 current sensing transformer and a 910Ω resistor. The feedforward gain from the input voltage is K_f=*-0.00341*. The feedback gains from the outputs are K_{r1}=*-0.027* and K_{r2}=*-0.015*. Since the control-to-feedback transfer function, shown in Fig. 9, has interlaced poles and zeros, a compensator with an integrator plus one pole and one zero is employed:

$$A_c(s)=\frac{K_I\ (1+s/s_z)}{s\ (1+s/s_p)}, \tag{23}$$

where the integrator gain K_I=*99920 rad./s.*, the compensator zero s_z=*62858 rad./s.*, and the compensator pole z_p=*502810 rad./s.*.

V. Summary

In this paper, a small-signal model for current-mode control is derived. The derivation is based on the generic

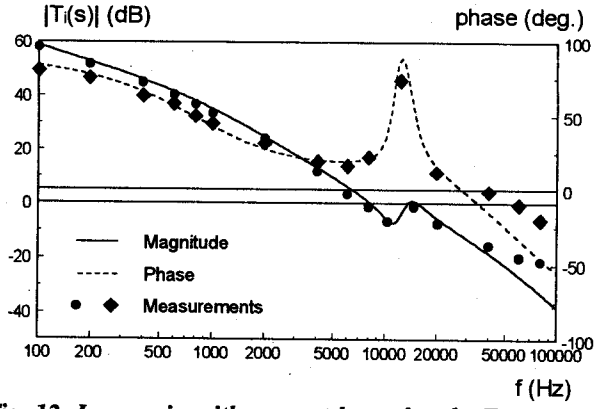

Fig. 12. Loop gain with current-loop closed. *For current-mode control, the problem of multiple-crossing of the 0 dB line also exists due to the multiple peaks of the power stage transfer functions. Fortunately, the phase delay in this vicinity is not significant, and therefore it will not cause stability problem.*

current cell which is universal regardless of the specific topology dealt with. The effects of the perturbations of the input and output voltages on the feedback current are characterized by the feedforward gain, K_f, and feedback gains, K_{r1} and K_{r2}.

The derived small-signal model can accurately predict some unique characteristics for current mode control such as subharmonic oscillation. Like a single output converter, the low frequency double poles of the power stage transfer function for a MOC with current mode control are split into two single poles, which make the power stage transfer function behave like a single pole system at low frequency. The extra pole-zero pair of the MOC, however, still exhibits multiple peaks.

When designing the compensator for a MOC, the relative positions of the power stage duty cycle-to-feedback transfer function with current loop closed are important in determining the type of the compensator. For a pole-zero interlaced system, an integrator plus one pole and one zero is a good candidate. For pole-zero non-interlaced system, an integrator has to be used to ensure stability of the system, but nonetheless this situation is undesirable. Since the pole-zero interlacing relationship, as given in [7], is not changed by introducing current-mode control, it can be employed to design a pole-zero interlaced system.

References

[1] M. Goldman and A. Witulski, "Predicting Regulation for a Multiple-Output Current-Mode controlled Dc-to-Dc Converter," *Proc. IEEE Applied Power Electronics Conf.*, March 1993, pp. 617-623.

[2] Q. Chen, F.C. Lee, and M.M. Jovanovic, "Small-Signal Analysis and Design of Weighted Voltage Control for a Multiple-Output Forward Converter," *IEEE Power Electronics Specialists Conf. Rec.*, 1993, pp. 749-756.

[3] A. Brown, "Topics in the Analysis, Measurement, and Design of High-Performance Switching Regulators," Ph.D. Dissertation, California Institute of Technology, Department of Electrical Engineering, Pasadena, California, 1981.

[4] F. C. Lee and A. R. Carter, "Investigation of Stability and Dynamic Performance on Switching Regulators Employing Current-Injected Control," *IEEE Power Electronics Specialists Conf. Rec.*, 1981, pp. 3-16.

[5] R. D. Middlebrook, "Topics in Multiple-Loop Regulators and Current-Mode Programming," *IEEE Trans. Power Electronics*, vol. 2, no. 2, pp. 109-124, 1987.

[6] R. Ridley, "A New Small-Signal Model for Current-Mode Control," Ph.D. Dissertation, Virginia Polytechnic Institute and State University, Blacksburg, Virginia, Nov. 27, 1990.

[7] Q. Chen, "Analysis and Design of Multiple-Output Forward Converter with Weighted-Voltage Control," Ph.D. Dissertation, Virginia Polytechnic Institute and State University, Blacksburg, Virginia, Feb. 9, 1994.